Double-slit experiment at Fermi scale: Coherent photoproduction in heavy-ion collisions

W. Zha,[1,*] L. Ruan,[2] Z. Tang,[1,†] Z. Xu,[2,3] and S. Yang[2]

[1]*Department of modern physics, University of Science and Technology of China, Hefei 230026, China*
[2]*Brookhaven National Laboratory, New York 11973, USA*
[3]*Shandong University, Jinan 250100, China*

The double-slit experiment has become a classic thought experiment for its clarity in expressing the central puzzle of quantum mechanics—wave-particle complementarity. Such wave-particle duality continues to be challenged and investigated in a broad range of entities with electrons, neutrons, helium atoms, C_{60} fullerenes, Bose-Einstein condensates, and biological molecules. In this Rapid Communication, we present a double-slit scenario at Fermi scale with new entities—coherent photon products in heavy-ion collisions. Virtual photons from the electromagnetic fields of relativistic heavy ions can fluctuate to quark-antiquark pairs, scatter off a target nucleus, and emerge as vector mesons. The two colliding nuclei can take turns to act as targets, forming a double-slit interference pattern. Furthermore, the "which-way" information can be partially solved using sufficiently-high multiplicity heavy-ion collisions so that the reaction plane can be determined, which demonstrates the complementary principle, a key concept of quantum mechanics.

Relativistic heavy ions carry giant electromagnetic fields which can be equivalent to a field of quasireal virtual photons [1]. When two ions collide, the photon from the field of one nucleus may fluctuate into a virtual quark-antiquark pair which scatters elastically from the other nucleus, emerging as a real vector meson. The elastic scattering occurs via short-range strong force, which imposes a restriction on the production site of a vector meson within one of the two ions. This provides the production process with a choice: Either nucleus 1 emits a virtual photon, whereas nucleus 2 acts as a target or vice versa. If the information is missing about which nucleus emits a photon or acts as the target, the vector meson, behaving as a wave, originates simultaneously from both colliding nuclei. The wavelike behavior and corresponding interference present themselves as a perfectly double-slit experiment of individual particles. The double-slit experiment has become a classic thought experiment for its clarity in expressing the central puzzle of quantum mechanics—wave-particle complementarity. Such wave-particle duality [2] continues to be challenged [3–7] and investigated in a broad range of entities with electrons [8], neutrons [9], helium atoms [10], C_{60} fullerenes [11], Bose-Einstein condensates [12], and biological molecules [13]. In this Rapid Communication, we demonstrate that the coherent photoproduction in heavy-ion collisions could extend the double-slit scenario to Fermi scale with new entities—vector mesons [14]. Furthermore, the violent hadronic interactions accompanied by heavy-ion collisions could partially solve the "which-slits" problem, leading to the appearance of decoherence, which demonstrates a key concept of quantum mechanics—complementary principle.

In contrast to the light vector mesons, photoproduction of heavy vector mesons offers an opportunity to directly determine the gluon distributions in nucleons and nuclei [15], which are not directly accessible in deep inelastic scattering. Due to their clarity in the physical picture and experimental feasibility, we choose J/ψ, the most abundant heavy vector meson, as the entity to illustrate the double-slit scenario in heavy-ion collisions. The J/ψ photoproduction from the two nuclei is related by a parity transformation, and the parity of J/ψ is negative, which assigns the amplitudes from the two directions with opposite signs. This gives the presented double-slit scenario a unique feature—a phase shift of π between the two interference sources. Furthermore, the probability of multiple J/ψ production in one collision is negligible in comparison with that of single production, which indicates that the interference pattern is built up one by one in the proposed scenario. This is an important version of double-slit experiments to clearly demonstrate the wave-particle duality, which states that all matter exhibits both wave and particle properties.

In heavy-ion collisions, the momentum of J/ψ can be reconstructed by the detectors, which allows us to observe the interference fringes in momentum space. The probability distribution of J/ψ in momentum space can be calculated by performing a Fourier transformation to the amplitude in coordinate space, defined as

$$\frac{d^2P}{dp_x dp_y} = \frac{1}{2\pi} \left| \int d^2r \left[A_1\left(y, \mathbf{r}, -\frac{b}{2}\right) + A_2\left(y, \mathbf{r}, \frac{b}{2}\right) \right] e^{i\mathbf{p}\cdot\mathbf{r}} \right|^2,$$

(1)

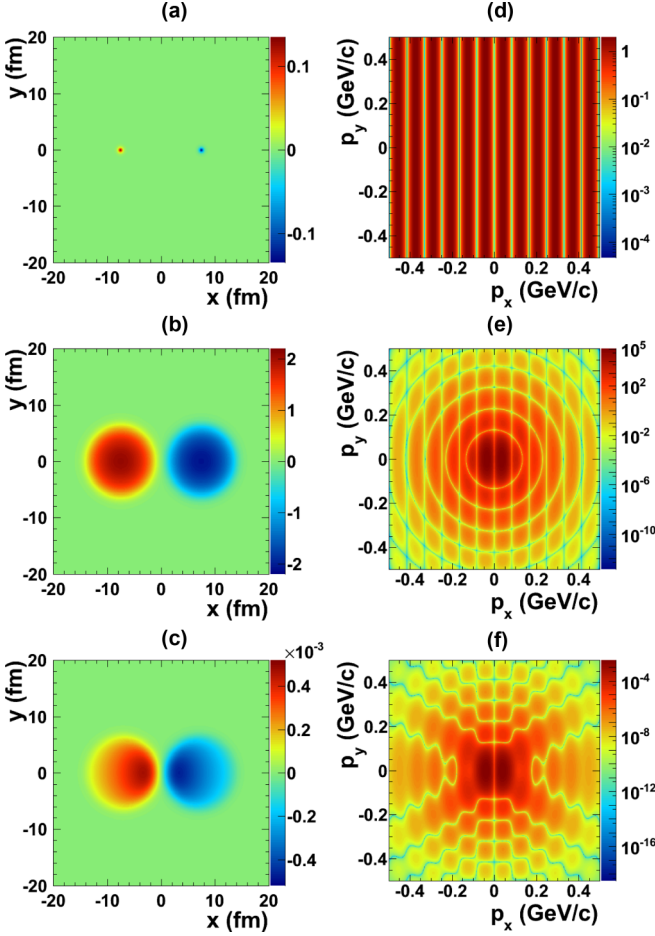*wangmei@rcf.rhic.bnl.gov
†zbtang@ustc.edu.cn

FIG. 1. Amplitude and momentum distribution patterns of coherent J/ψ photoproduction with different scenarios for $b = 15$ fm at midrapidity ($y = 0$). Panel (a): point source scenario, panel (b): Woods-Saxon distribution, and panel (c): realistic scenario described in the text. Panels (d)–(f) show the corresponding momentum distributions according to the amplitude scenarios in panels (a)–(c), respectively.

where $A_1(y, \mathbf{r}, -\frac{b}{2})$ and $A_2(y, \mathbf{r}, \frac{b}{2})$ are the amplitudes with rapidity y for J/ψ production at distant $\mathbf{r}$ from the two colliding nuclei, respectively; b is the slit separation, which is the so-called impact parameter in heavy-ion collisions. We take $\hbar = c = 1$ here. The J/ψ production is coherent over the entire nucleus, for a start, we approximate the production regions as two point sources, one at the center of each nucleus. At midrapidity ($y = 0$), the magnitudes of amplitudes from the two directions are the same. With the point source assumption, the amplitudes from nuclei 1 and 2 at midrapidity can be written as

$$A_1\left(0, \mathbf{r}, -\frac{b}{2}\right) = \delta\left(r + \frac{b}{2}\right), \quad A_2\left(0, r, \frac{b}{2}\right) = -\delta\left(r - \frac{b}{2}\right). \tag{2}$$

Here, $\delta(x)$ is the Dirac δ function. The amplitude distribution in coordinate space and the corresponding interference pattern in momentum space with slit separation $b = 15$ fm are shown in Fig. 1 panels (a) and (d), respectively. The momentum

distribution reveals a typical Young's double-slit interference pattern with a series of alternating light and dark fringes. The width of the fringes reflects the distant between the two slits: $d = \frac{2\pi}{b}$. The straight fringes exhibit the central minimum due to the opposite sign amplitudes from the two sources. For the more realistic case, the two nuclei (slits) possess certain sizes and profiles at Fermi scale. The density profile of the nucleus can be parametrized by the Woods-Saxon distribution,

$$\rho_A(r) = \frac{\rho^0}{1 + \exp[(r - R_{\mathrm{WS}})/d]}, \tag{3}$$

where the radius R_{WS} and skin depth d are based on fits to electron-scattering data [17] and ρ^0 is the normalization factor. With $A(\mathbf{r}) = T(\mathbf{r}) = \int_{-\infty}^{+\infty} \rho(\sqrt{r^2 + z^2})dz$, the amplitude distribution in coordinate space and the corresponding momentum distribution for Au + Au collisions are shown in panels (b) and (e), respectively. Due to the profile of slits, typical diffraction rings emerge on top of the interference fringes in momentum distribution. The diffraction, a multiple-slit interference, has the equivalent ability as a double-slit experiment to demonstrate wave-particle duality, which could be further investigated in the future electron-ion collider [18]. The amplitudes in coordinate space are further modified by the spatial photon flux, nuclear shadowing, and coherent length effects. The spatial photon flux induced by ions can be given by the equivalent photon approximation [1],

$$\frac{d^3 N_\gamma(\omega_\gamma, \vec{x}_\perp)}{d\omega_\gamma d\vec{x}_\perp} = \frac{4Z^2\alpha}{\omega_\gamma} \left| \int \frac{d^2\vec{k}_{\gamma\perp}}{(2\pi)^2} \vec{k}_{\gamma\perp} \frac{F_\gamma(\vec{k}_\gamma)}{|\vec{k}_\gamma|^2} e^{i\vec{x}_\perp \cdot \vec{k}_{\gamma\perp}} \right|^2,$$

$$\vec{k}_\gamma = \left(\vec{k}_{\gamma\perp}, \frac{\omega_\gamma}{\gamma_c}\right), \quad \omega_\gamma = \frac{1}{2}M_{J/\psi}e^{\pm y}, \tag{4}$$

where $\vec{x}_\perp$ and $\vec{k}_{\gamma\perp}$ are two-dimensional photon position and momentum vectors perpendicular to the beam direction, Z is the nuclear charge, α is the electromagnetic coupling constant, γ_c is the Lorentz factor of the photon-emitting nucleus, $M_{J/\psi}$ and y are the mass and rapidity of J/ψ, and $F_\gamma(\vec{k}_\gamma)$ is the nuclear electromagnetic form factor. $F_\gamma(\vec{k}_\gamma)$ is obtained via the Fourier transformation of the charge density in the nucleus. The calculation of scattering amplitude $\Gamma_{\gamma A \to J/\psi A}(\mathbf{r})$ with the shadowing effect can be performed with quantum Glauber [19] + vector meson dominance (VMD) approach [20] coupled with the parametrized forward-scattering amplitude $f_{\gamma p \to J/\psi N}(0)$ [21] as input,

$$\Gamma_{\gamma A \to J/\psi A}(\mathbf{r}) = \frac{f_{\gamma p \to J/\psi N}(0)}{\sigma_{J/\psi N}} 2\left[1 - \exp\left(-\frac{\sigma_{J/\psi N}}{2}T'(\mathbf{r})\right)\right]. \tag{5}$$

Using the optical theorem and VMD relation, the total cross section for $J/\psi N$ scattering is given by

$$\sigma_{J/\psi N} = \frac{f_{J/\psi}}{4\sqrt{\alpha}C} f_{\gamma p \to J/\psi N}(0), \tag{6}$$

where $f_{J/\psi}$ is the J/ψ-photon coupling and C is a correction factor for the nondiagonal coupling through higher mass vector mesons [22]. To account for the coherent length effect,

$T'(\mathbf{r})$ is defined as

$$T'(\mathbf{r}) = \int_{-\infty}^{+\infty} dz \rho(\sqrt{\mathbf{r}^2 + z^2}) e^{iq_L z}, \quad q_L = \frac{M_{J/\psi} e^y}{2\gamma}, \quad (7)$$

where q_L is the longitudinal momentum transfer required to produce a real J/ψ. With these effects, the amplitude from one direction can be written as

$$A_1\left(y, \mathbf{r}, -\frac{b}{2}\right) = \Gamma_{\gamma A \to J/\psi A}\left(\mathbf{r} + \frac{\mathbf{b}}{2}\right) \sqrt{\frac{d^2 N_\gamma\left(\mathbf{r} + \frac{\mathbf{b}}{2}\right)}{d^2 r}}, \quad (8)$$

which makes the slits become asymmetric. The amplitude distributions of the asymmetric slits in Au + Au collisions at $\sqrt{s_{NN}} = 200$ GeV for midrapidity ($y = 0$) are shown in Fig. 1, panel (c), and the resulting interference pattern is depicted in panel (f). The corresponding diffraction pattern does not show typical symmetric diffraction rings due to the asymmetric profile of slits, and the interference fringes become curving.

The coherent photoproduction has been studied in detail in ultraperipheral collisions (UPCs) [14] in which the impact parameter is larger than twice the nuclear radius. The destructive interference of ρ^0 in transverse momentum for UPCs has been proposed by Klein and Nystrand [23] and verified by the STAR Collaboration [24]. However, no special azimuthal direction can be determined in UPCs, which prevents us from observing the two-dimensional interference fringes. Fortunately, in hadronic heavy-ion collisions (HHICs) when the two nuclei overlap, the reaction plane, spanned by the impact parameter and the beam axis, can be estimated from the azimuthal anisotropy of produced particles due to the asymmetric geometry in the overlap region. Herein, the disruption to interference action from the violent hadronic interactions in the overlap region is ignored, which would be discussed in detail in the latter. Furthermore, in HHICs, the impact parameter (centralities) could be precisely determined, which allows us to vary the slit separation in the presented scenario. The profile of amplitudes and the corresponding momentum distributions in Au + Au collisions at $\sqrt{s_{NN}} = 200$ GeV with different slit separations at midrapidity ($y = 0$) are shown in Fig. 2. In this Rapid Communication, P_x is defined to be parallel to the reaction plane on the transverse plane, whereas P_y is perpendicular to the reaction plane. As demonstrated in the figure, the bandwidth of interference fringes becomes wider when the slit separation gets smaller. And the diffraction pattern changes due to the different profiles of slits with different slit separations. In the proposed scenario, the relative brightness between the two slits could also be adjusted by detecting the coherently produced J/ψ's at different rapidities. Figure 3 shows the amplitude distributions and the corresponding momentum distributions in Au + Au collisions at $\sqrt{s_{NN}} = 200$ GeV with the slit separation $b = 10$ fm for the J/ψ production at different rapidities. When going to forward rapidities due to the dominant production from one direction, the interference fringes merge into each other, which makes the diffraction pattern dominant over the momentum distributions.
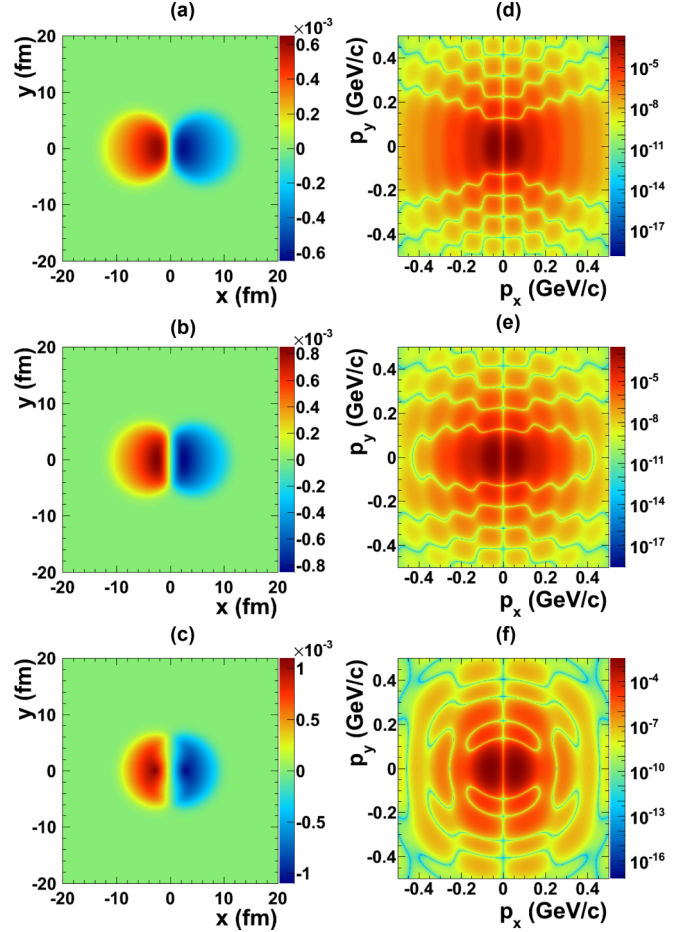

FIG. 2. Amplitude and momentum distribution patterns of coherent J/ψ photoproduction in Au + Au collisions at $\sqrt{s_{NN}} = 200$ GeV for midrapidity ($y = 0$) with different impact parameters. Panels (a) and (d): $b = 13.0$ fm, panels (b) and (e): $b = 10.0$ fm, and panels (c) and (f): $b = 5.7$ fm.

A well-known double-slit thought experiment predicts that, if particle detectors are positioned at the slits to solve the "which-way" problem, the interference pattern will disappear, which illustrates the complementary principle that matter can behave as either particles or waves but cannot possess both at the same time. Conventional wisdom says that, in HHICs, the strong interactions and possible quark-gluon-plasma [25] in the overlap region detect the coherently produced J/ψ's and determine the which-way information, leading to decoherence, which prohibits the coherent photoproduction. However, the ALICE [16] and STAR [26] Collaborations observed significant anomaly excesses of J/ψ production in HHICs at very low transverse momentum ($p_T < 0.3$ GeV/c), which could be qualitatively described by the coherent photoproduction mechanism [27]. The strong evidence of the existence of coherent photoproduction in HHICs help us to consider the disruption from the overlap region more carefully. The strong interactions are short range, so they cannot observe or detect the coherent photoproduction out of the hot medium region. The which-way information is only obtained within the extent of strong interactions, which means that the which-
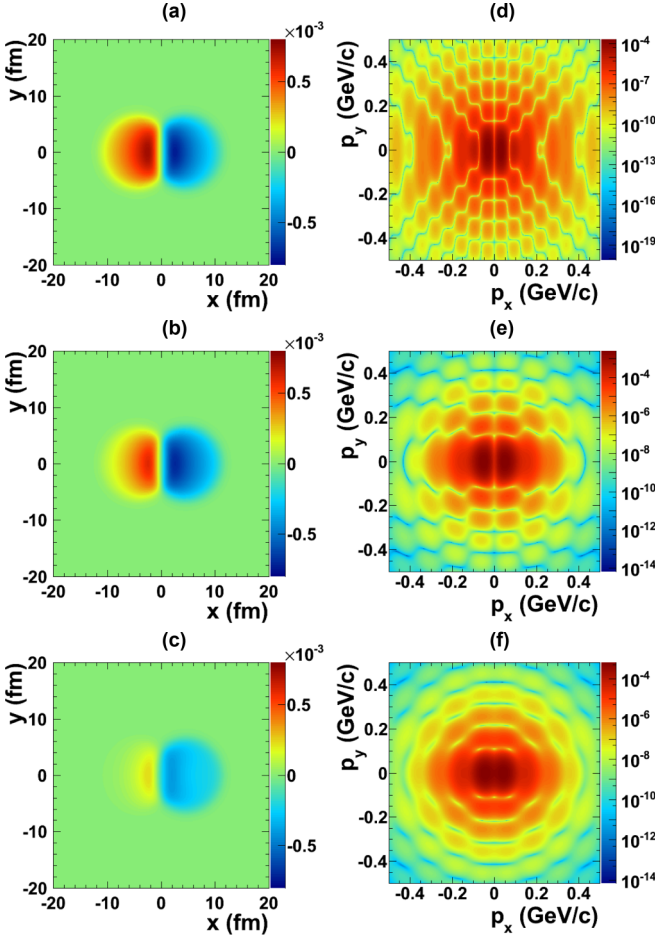
FIG. 3. Amplitude and momentum distribution patterns of coherent J/ψ photoproduction in Au + Au collisions at $\sqrt{s_{NN}} = 200$ GeV with $b = 10.0$ fm at different rapidities. Panels (a) and (d): $y = 0.0$, panels (b) and (e): $y = 0.6$, and panels (c) and (f): $y = 1.4$.
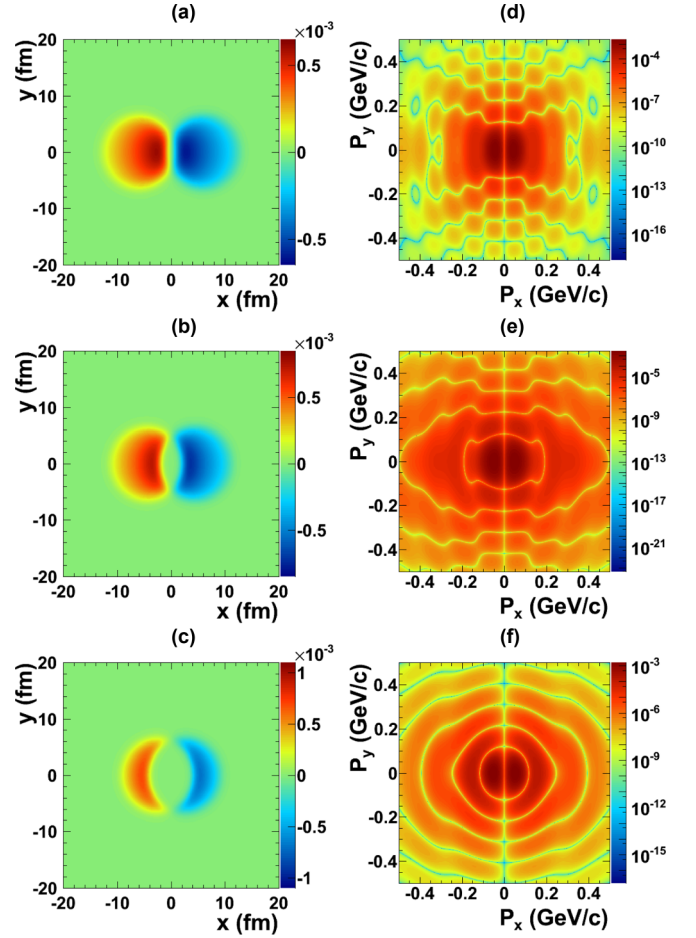

FIG. 4. Amplitude and momentum distribution patterns of coherent J/ψ photoproduction at midrapidity ($y = 0$) in Au + Au collisions at $\sqrt{s_{NN}} = 200$ GeV with a disruption effect from overlap region for different impact parameters. Panels (a) and (d): $b = 13.0$ fm, panels (b) and (e): $b = 10.0$ fm, and panels (c) and (f): $b = 5.7$ fm.

slit problem is only partially solved, or the two slits are only sectionally blocked by the interactions but not all. Herein, we adopt a simple assumption that the which-way information is only obtained in the initial overlap region. The violent interactions in the overlap region may impose impact on the photon emission. Due to the time-retarded potential, the quasireal photons are likely to be emitted before hadronic collision by about $\Delta t = \gamma R/c$, where γ is the Lorentz factor, and R is the transverse distance from the colliding nuclei. Hence, the photon emission should be unaffected by hadronic collisions. The remanent part of the nuclei (spectators) would fragment, which may also modify the profile of the two slits. However, the effect should be negligible since the fragment timescale is far more longer than that of J/ψ production. The amplitude distributions of the sectional blocked slits and the corresponding momentum distribution patterns in Au + Au collisions at $\sqrt{s_{NN}} = 200$ GeV with different impact parameters at midrapidity are depicted in Fig. 4. In comparison with the interference and diffraction patterns shown in Fig. 2, the diffraction rings and interference fringes change significantly due to the partial blocking of the slits. The integrated yields of coherent J/ψ production as a function of N_{part} with the whole slits

and sectional blocked slits ("observation" effect) are shown in Fig. 5 for Au + Au collisions at (a) $\sqrt{s_{NN}} = 200$ GeV and (b) Pb + Pb collisions at $\sqrt{s_{NN}} = 2.76$ TeV. The integrated production rate is significantly reduced by the observation effect in the semicentral and central collisions. And in comparison with the experimental measurements from the ALICE [16] and STAR [26] Collaborations, the data seem to favor the calculation with the observation effect, however, could not distinguish the two scenarios due to limited statistics.

By making use of the coherent photoproduction in HHICs, one can take Young's famous experiment one step further at Fermi scale and create a truly one-by-one double-slit setup composed of new entities—the vector meson. The slit separations and relative brightness between slits can be adjusted in the presented scenario. In addition, the strong interactions in the overlap region detect the coherent products and partially solve the which-way information, which serves as a good double-slit scenario to test the observation effect on wave-particle duality and further demonstrates the complementary principle.
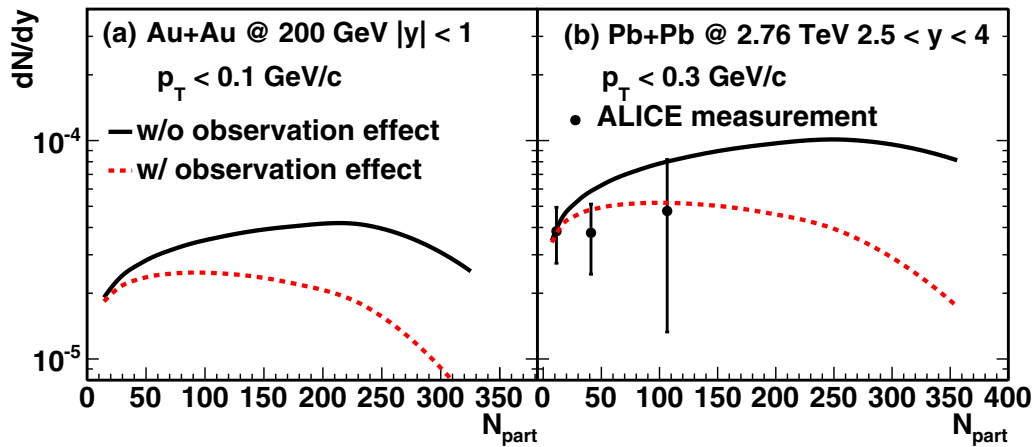
FIG. 5. Integrated yields of coherent J/ψ production with and without an "observation" effect as a function of N_{part} in (a) Au + Au collisions at $\sqrt{s_{\mathrm{NN}}} = 200$ GeV and (b) Pb + Pb collisions at $\sqrt{s_{\mathrm{NN}}} = 2.76$ TeV. Data from the experiment of the ALICE Collaboration [16] are shown for comparison.

[1] F. Krauss, M. Greiner, and G. Soff, Prog. Part. Nucl. Phys. **39**, 503 (1997).

[2] L. De Broglie, Nature (London) **112**, 540 (1923).

[3] M. O. Scully, B.-G. Englert, and H. Walther, Nature (London) **351**, 111 (1991).

[4] H. Wiseman and F. Harrison, Nature (London) **377**, 584 (1995).

[5] F. Lindner *et al.*, Phys. Rev. Lett. **95**, 040401 (2005).

[6] M. Kiffner, J. Evers, and C. H. Keitel, Phys. Rev. Lett. **96**, 100403 (2006).

[7] B. King, A. Di Piazza, and C. H. Keitel, Nat. Photonics **4**, 92 (2010).

[8] C. Jönsson, Z. Phys. **161**, 454 (1961).

[9] A. Zeilinger *et al.*, Rev. Mod. Phys. **60**, 1067 (1988).

[10] O. Carnal and J. Mlynek, Phys. Rev. Lett. **66**, 2689 (1991).

[11] M. Arndt *et al.*, Nature (London) **401**, 680 (1999).

[12] M. R. Andrews *et al.*, Science **275**, 637 (1997).

[13] L. Hackermüller, S. Uttenthaler, K. Hornberger, E. Reiger, B. Brezger, A. Zeilinger, and M. Arndt, Phys. Rev. Lett. **91**, 090408 (2003).

[14] C. A. Bertulani, S. R. Klein, and J. Nystrand, Annu. Rev. Nucl. Part. Sci. **55**, 271 (2005).

[15] V. Guzey and M. Zhalov, J. High Energy Phys. 10 (2013) 207.

[16] J. Adam *et al.* (ALICE Collaboration), Phys. Rev. Lett. **116**, 222301 (2016).

[17] R. C. Barrett and D. F. Jackson, *Nuclear Sizes and Structure* (Oxford University Press, Oxford, 1977) .

[18] A. Accardi *et al.*, Eur. Phys. J. A **52**, 268 (2016).

[19] M. L. Miller *et al.*, Annu. Rev. Nucl. Part. Sci. **57**, 205 (2007).

[20] T. H. Bauer *et al.*, Rev. Mod. Phys. **50**, 261 (1978).

[21] S. R. Klein *et al.*, Comput. Phys. Commun. **212**, 258 (2017).

[22] J. Hufner and B. Z. Kopeliovich, Phys. Lett. B **426**, 154 (1998).

[23] S. R. Klein and J. Nystrand, Phys. Rev. Lett. **84**, 2330 (2000).

[24] B. I. Abelev *et al.* (STAR Collaboration), Phys. Rev. Lett. **102**, 112301 (2009).

[25] P. Braun-Munzinger and J. Stachel, Nature (London) **448**, 302 (2007).

[26] W. Zha (STAR Collaboration), J. Phys.: Conf. Ser. **779**, 012039 (2017).

[27] W. Zha *et al.*, Phys. Rev. C **97**, 044910 (2018).